X-Ray and Neutron Diffraction Studies on Amorphous Transitionmetal — Boron Alloys (Fe-B, Co-B, Ni-B)

P. Lamparter, E. Nold, G. Rainer-Harbach, E. Grallath, and S. Steeb

Max-Planck-Institut für Metallforschung, Institut für Werkstoffwissenschaften, Stuttgart Germany

Z. Naturforsch. **36a**, 165–172 (1981); received December 11, 1980

The atomic-scale structure of the amorphous metallic alloys $Fe_{80}B_{20}$, $Co_{81.5}B_{18.5}$, and $Ni_{81.5}B_{18.5}$ was investigated by X-ray- and neutron-diffraction covering a wide range of the ratio (f_{metal}/f_{boron}) of the scattering factors of both components. The structure factors $S(q)$ show a pronounced dependence on the ratio f_{metal}/f_{boron}. In the cases of a small ratio an additional peak near $q = 21.5$ nm^{-1} appears in the structure factors from which a definite distance between B-B atoms, which are separated by metal atoms, is deduced. The corresponding structure factors show only weak oscillations in the range of the second and third maxima, which are followed by increased amplitudes at larger q's.

By Fourier-transformation radial distribution curves were evaluated, from which the distances between the metal-metal-, the metal-boron-, and the boron-boron-atoms and the coordination numbers are extracted. From the splitted first maximum of the radial distribution function in the cases of small ratio f_{metal}/f_{boron} also partial coordination numbers could be obtained. The results suggest some kind of short range order between the metal and the boron atoms.

Introduction

The elucidation of the atomic-scale structure of an amorphous metal-metalloid alloy requires the knowledge of three partial atomic distribution functions describing the correlations between the metal-metal, metalloid-metalloid, and the metal-metalloid atoms. At least three scattering experiments are needed where the ratios of the scattering factors differ. This can be achieved by the isotopic substitution technique for neutron diffraction, where the scattering factor of at least one component is altered by using different isotopes in preparing samples with identical chemical composition. Another method is the combination of X-ray and neutron diffraction measurements where the scattering factors are different. A further method is the so called isomorphous substitution of one component by an element with another scattering factor, assuming no remarkable alteration of the structure.

In the present work these three methods were employed for the investigation of the structure of $T_{80}B_{20}$-type metallic glasses (T=Fe, Co, Ni) in order to cover a wide range of the ratio of the scattering factors of the T metal and boron varying from 5.60 to 0.46.

Reprint requests to Prof. Dr. S. Steeb, Max-Planck-Institut f. Metallforschung, Institut für Werkstoffwissenschaften, Seestraße 92, 7000 Stuttgart 1.

Experimental Procedures and Evaluation of the Structure Factors

Preparation

The amorphous samples were prepared as ribbons with a thickness of about 0.03 mm by rapidly quenching the molten alloys using the melt spinning technique. The compositions of the samples are listed in Table 1. As the B component the ^{11}B isotope had to be used because B with natural isotopic abundance is an extremely strong neutron absorber.

Structure Factor

During the present work the structure factors $S(q)$ according to the Faber Ziman definition were used:

$$S(q) = [I_{coh}(q) - \mathrm{LMS}]/\langle f\rangle^2 , \qquad (1)$$

where

q = $4\pi \sin\theta/\lambda$ = total of the scattering vector $\boldsymbol{q}$,
2θ = scattering angle,
λ = wavelength of the radiation,
$I_{coh}(q)$ = coherently scattered intensity per atom,
$\langle f\rangle$ = $c_1 f_1 + c_2 f_2$,
c_1, c_2 = atomic concentration of the component 1, 2,
f_1, f_2 = scattering factor of the component 1, 2,
LMS = $\langle f^2\rangle - \langle f\rangle^2$ = Laue monotonic scattering.

0340-4811 / 81 / 0200-0165 $ 01.00/0. — Please order a reprint rather than making your own copy.

Table 1. Relevant parameters of the investigated samples. f_T/f_B = ratio of the scattering factors, q^I[nm^{-1}], $S(q^I)$ = position and height of the principal peak of the structure factor. $r_{ij}^{n,m}$[nm = distance of a j-type atom within the m-th subpeak in the n-th coordination shell from a i-type atom. Values in brackets are normalized to $r_{TT}^{I,2}$. N_m^I = measured area below the first peak of the RDF(r). N_c^I = calculated area below the first peak of the RDF(r). z_{ij} = partial coordination number of j-type atoms around an i-type atom.

Sample radiation; λ[nm]	Density [g/cm^3]	$\frac{f_T}{f_B}$	q^I $S(q^I)$	Maximum I		Maximum II				Maximum III			N_m^I N_c^I	z_{TT} z_{TB} z_{BT}
				$r_{BT}^{I,1}$	$r_{TT}^{I,2}$	$r^{II,1}$	$r_{TT}^{II,2}$	$r_{BT}^{II,3}$	$r_{TT}^{II,4}$	$r^{III,1}$	$r_{TT}^{III,2}$	$r^{III,3}$		
$Co_{81.5}B_{18.5}$	8.3	5.40	31.8		0.251		0.417		0.482		0.625		14.3	
X-ray, Mo-K_α; 0.071			4.44				(1.66)		(1.92)		(2.49)		15.0	
$Fe_{80}B_{20}$	7.31	5.20	31.2		0.257		0.416		0.498		0.635		14.6	
X-ray, Mo-K_α; 0.071			3.80				(1.62)		(1.94)		(2.47)		14.1	
$Ni_{81.5}B_{18.5}$	8.36	1.72	31.8		0.250		0.416		0.482		0.631		13.9	
neutron; 1.03			3.80				(1.66)		(1.93)		(2.52)		—	
$^{nat}Fe_{80}B_{20}$	7.31	1.58	31.3		0.258		0.417		0.495		0.642		14.2	
neutron; 0.69			3.63				(1.62)		(1.92)		(2.49)		13.4	
$^{57}Fe_{80}B_{20}$	7.31	0.69	31.7	0.213	0.255	0.367	0.409	0.440	0.505	0.59	0.629	0.67		11.5
neutron; 0.69			2.86	(0.835)		(1.44)	(1.60)	(1.73)	(1.98)	(2.31)	(2.47)	(2.63)		2.2
														8.9
$Co_{81.5}B_{18.5}$	8.3	0.46	32.3	0.207	0.250	0.360	0.406	0.437	0.485	0.585	0.626	0.67		12.7
neutron; 0.79, 2.42			2.97	(0.828)		(1.44)	(1.62)	(1.75)	(1.94)	(2.34)	(2.50)	(2.68)		1.5
														6.6

X-Ray Diffraction with $Co_{81.5}B_{18.5}$ and $Fe_{80}B_{20}$

The X-ray diffraction experiments with $Co_{81.5}B_{18.5}$ and $Fe_{80}B_{20}$ were carried out in transmission mode with Mo-K_α radiation from a 12 kW rotating anode X-ray generator and a graphite monochromator in the primary beam. Suitable corrections of the measured intensities were done as described in previous studies [1, 2]. After the normalization of the corrected data with the Krogh Moe method [3] the structure factors $S(q)$ were derived.

Neutron Diffraction with $Co_{81.5}B_{18.5}$ and $Ni_{81.5}B_{18.5}$

The neutron diffraction experiments with $Co_{81.5}B_{18.5}$ and $Ni_{81.5}B_{18.5}$ were performed with the two axis powder diffractometer P14 at the research reactor FR2, Kernforschungszentrum Karlsruhe. The specimens were prepared by cutting 10 grams of the amorphous ribbon into small shreds and pressing them randomly oriented into a vanadium tube with 0.1 mm wall thickness. This yielded specimens with 42 mm height and 5.7 mm diameter.

The sample containing Ni was measured with the neutron wavelength of 0.103 nm in the q range from 10 up to 104 nm^{-1}. For the sample containing Co two scattering experiments with the wavelengths 0.0787 nm and 0.242 nm, respectively, were performed in order to cover a more extended q range up to 137 nm^{-1}. The step scan width was 0.25°. Due to the very small scattering factor of Co, 20 days had to be expended to collect 10^4 counts per measured point on an average.

For the background- and the absorption correction of the measured data the Paalman Pings method [4] was applied. For the evaluation of the structure factors from the corrected intensities the magnetic scattering of the transition metals had to be taken into consideration.

The magnetic moments of Fe, Co, and Ni give rise to a q-dependent magnetic scattering intensity $I_m(q) = P^2(q)\, S(q) \sin^2\alpha$, $P(q)$ being the magnetic scattering length which exists besides the nuclear scattering factors f [5]:

$$P(q) = (r_0\gamma/2)\,\mu F(q)\,, \qquad (2)$$

where r_0 is the classical electron radius ($2.8 \cdot 10^{-13}$ cm), γ the neutron magnetic moment (-1.91), μ the atomic magnetic moment, α the angle between the atomic moment and the scattering vector $\boldsymbol{q}$, and $F(q)$ the magnetic form factor, which is normalized to one for $q=0$ and decreases to zero with increasing q.

$Ni_{81.5}B_{18.5}$

For the case of the $Ni_{81.5}B_{18.5}$-alloy, the magnetic scattering could be neglected because the magnetic moment of Ni is nearly zero in an alloy containing 18.5% B [6]. So the corrected intensity data

were normalized by the Krogh Moe method [3] to obtain the coherent scattering per atom yielding the structure factor $S(q)$ using (1). The multiple scattering correction was done corresponding to [7].

$Co_{81.5}B_{18.5}$

For the case of the $Co_{81.5}B_{18.5}$-alloy, the magnetic moment of the Co atoms was taken as 1.08 Bohr magnetons [6]. The magnetic scattering contribution of the Co atoms was calculated as follows:

The measurement with the $Co_{81.5}B_{18.5}$ sample was carried out with non-polarized neutrons and without an external magnetic field, so that the magnetic moments of the Co atoms were orientated randomly. For this set up the magnetic scattering contribution is associated only with the correlation among the Co atoms, that means the partial Co-Co structure factor $S_{\mathrm{CoCo}}(q)$, and it can be written as [5]

$$I_{\mathrm{m}}(q) = \tfrac{2}{3} P^2(q) S_{\mathrm{CoCo}}(q) . \tag{3}$$

The total scattered intensity is then

$$I_{\mathrm{t}}(q) = I_{\mathrm{coh,n}}(q) + I_{\mathrm{m}}(q) , \tag{4}$$

where $I_{\mathrm{coh,n}}$ means the coherent nuclear scattering.

As the magnetic form factor $F(q)$ decreases rapidly with increasing q, $I_{\mathrm{m}}(q)$ can be neglected for $q > 70\ \mathrm{nm}^{-1}$, and the normalization of the scattered intensity was done using the fact that $I_{\mathrm{t}}(q)$ oscillates around $\langle f^2 \rangle$ in the high q range. The calculation of $I_{\mathrm{m}}(q)$ with (3) was done presuming that the partial structure factor $S_{\mathrm{CoCo}}(q)$ is directly given by the structure factor $S(q)$ measured by an X-ray scattering experiment because the contribution of the B atoms is very small in this case. The form factor $F(q)$ was taken as applied successfully in the investigation of amorphous Co-P alloys by Blétry and Sadoc [8].

The calculated magnetic scattering contribution $I_{\mathrm{m}}(q)$ was subtracted from the normalized measured intensity $I_{\mathrm{t}}(q)$ thus yielding $I_{\mathrm{coh,n}}(q)$ and the structure factor $S(q)$ using (1).

Neutron Diffraction with $Fe_{80}B_{20}$

For the investigation of amorphous $Fe_{80}B_{20}$ by neutron diffraction the isotopic substitution method was applied. Using Fe of natural isotopic composition $^{\mathrm{nat}}$Fe in one case and iron enriched in the isotope ^{57}Fe (80.15% ^{57}Fe in Fe) in the other case two specimens were prepared. The diffraction experiments were carried out with the two axis diffractometer D4 at the Laue Langevin Institute, Grenoble, using non-polarized neutrons. For the elimination of the magnetic scattering contribution of the Fe atoms another method than that described for the case of Co was used: The amorphous ribbon was wound as a flat coil on a frame made of brass. To this specimen a magnetic field of 0.5 T parallel to the ribbons was applied, thus achieving magnetic saturation of the sample. With each of the two samples two diffraction experiments were performed. In the first run the magnetic field was parallel to the scattering vector. In this case α in (2) becomes zero and only the nuclear scattering $I_{\mathrm{coh,n}}(q)$ appears in the scattering pattern. For geometrical reasons the measurements with this set up could only done up to $q = 85\ \mathrm{nm}^{-1}$. In the second run the magnetic field was perpendicular to the scattering vector. For this case, the magnetic scattering contribution is

$$I_{\mathrm{m}}(q) = P^2(q) S_{\mathrm{FeFe}}(q) . \tag{5}$$

With this set up the measurements could be extended up to $q = 170\ \mathrm{nm}^{-1}$. Due to the q-dependence of the magnetic form factor $F(q)$ of Fe the magnetic contribution could be neglected in the q range beyond $70\ \mathrm{nm}^{-1}$. So the limited q range of the first run could be completed by the high q range of the second run, thus yielding the nuclear scattering $I_{\mathrm{coh,n}}(q)$ in the q range from 3 up to $170\ \mathrm{nm}^{-1}$ and the structure factor $S(q)$ with (1).

The densities of the amorphous specimens were taken from Ref. [9] and are listed in Table 1. The neutron scattering and absorption cross sections used for the data reduction are listed in Table 2.

Table 2. Neutron scattering and absorption cross sections as used in the present work. f = coherent scattering length, σ_{inc} = incoherent scattering cross section, σ_{a} = absorption cross section (listed for $\lambda = 0.108$ nm).

	f [10^{-12} cm]	σ_{inc} [10^{-24} cm^2]	σ_{a} [10^{-24} cm^2]
^{11}B	0.6	0	15.26
$^{\mathrm{nat}}$Fe	0.948	0.46	*
^{57}Fe	0.412	2.84	*
Co	0.278	5.04	21
Ni	1.03	4.8	2.7

* For these samples the total absorption was measured directly by a transmission experiment.

Results and Discussion

Structure Factors

Figure 1 shows the structure factors derived in the present work. They are plotted from the top to the bottom with decreasing ratio of the scattering factors of the transition metal (T) and the metalloid boron f_T/f_B. The curves a—d, where the scattering factor of the metal is greater than that of the metalloid, exhibit the behaviour often reported in the literature for amorphous metallic alloys, namely a double peak structure of the second maximum. In the case of the X-ray curves a and b, where the ratios f_T/f_B are nearly equal, it can be seen that the splitting of the second maximum is more pronounced with $Fe_{80}B_{20}$ than with $Co_{81.5}B_{18.5}$, and that the height of the principal peak is smaller with $Fe_{80}B_{20}$ (see also Table 1). The same effects can be observed with the neutron curves of $Fe_{80}B_{20}$(d) and $Ni_{81.5}B_{18.5}$(c), where the scattering factor ratios are again nearly equal.

It should be stressed that the differences between the curves a) and b) as well as between c) and d)

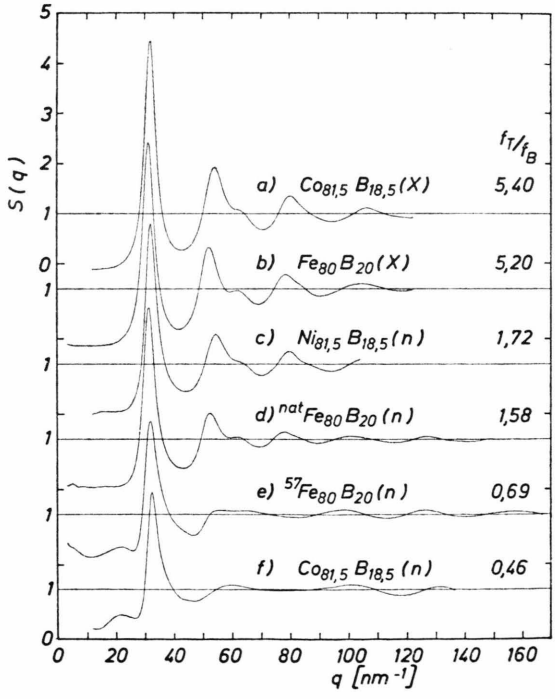

Fig. 1. Structure factors $S(q)$ of amorphous transition metal-boron alloys. f_T/f_B = ratio of the scattering factors of the metal and boron. (X) and (n) denote X-ray and neutron scattering, respectively.

cannot be explained by the uncertainties inherent to the diffraction experiment and the data reduction. Therefore there must be differences of the structure which can be caused either by the melt spin process, by the difference in the concentrations or by the replacement of the respective metals by another. This should be kept in mind when performing partial structure factor studies with the so called isomorphous substitution method.

The X-ray structure factor of $Fe_{80}B_{20}$ reported by Waseda and Chen [9] and also that reported by Suzuki et al. [10] for 19.6 at% B show only a shoulder at the high q side of the second maximum, whereas curve b of this work shows two separate peaks. The X-ray structure factor of $Fe_{80}B_{20}$ reported in Ref. [11] is in very good agreement with that one derived in the present work. The neutron structure factor obtained with $^{nat}Fe_{83}{}^{11}B_{17}$ in Ref. [12] shows much more pronounced amplitudes than that of curve d in Figure 1.

It should be noted that the X-ray structure factors of $Co_{81.5}B_{18.5}$ and $Fe_{80}B_{20}$ become negative in the low q region down to 3 nm^{-1}. This results from the definition of $S(q)$ (Eq. (1)), where the Laue monotonic term $(\langle f^2\rangle - \langle f\rangle^2)$ is subtracted. Because of the large difference of the X-ray scattering factors of boron and the T-metals this term is rather large. The physical presumption for calculating the LMS-term consists in the statistical distribution of both kinds of atoms on the atomic positions given by the corresponding structure. From the observation that the subtraction of the Laue monotonic scattering term leads to a negative value of $S(q)$ in this low q region it must be concluded that this physical presumption for the subtraction of the monotonic Laue scattering is not valid in the present case. This means that from the negative X-ray structure factors with $Fe_{80}B_{20}$ and $Co_{81.5}B_{18.5}$ we can deduce a *non* statistical distribution of the atoms of both kinds within these substances. In the present work we obtained for the Faber Ziman-structure factor in the low q region

$$Co_{81.5}B_{18.5}\text{(X-ray)}: S(q = 10\ nm^{-1}) = -0.11,$$

i.e. 79% of the Laue monotonic term, and

$$Fe_{80}B_{20}\text{(X-ray)}: S(q = 10\ nm^{-1}) = -0.125,$$

i.e. 84% of the Laue monotonic term.

With the $S(q)$ curves measured by neutron diffraction the effect discussed here is not visible be-

cause the Laue monotonic term becomes very small in this case.

Figure 1 (a—d) shows that the general features of $S(q)$ of the different samples and different radiation probes are very similar if $f_T/f_B > 1$. This behaviour is drastically changed (curves e and f) if $f_T/f_B < 1$. The neutron structure factors of $^{57}Fe_{80}B_{20}$ and $Co_{81.5}B_{18.5}$ are very similar: In front of the principal peak there occurs an additional peak at $q = 21.5 - 21.6\ nm^{-1}$. The principal peak is very low and the slight asymmetry at the right hand side noted already for the X-ray structure factors and assigned to a metal-metalloid-correlation in previous studies [9, 13] is very pronounced. The oscillations in the q range from 55 to 90 nm^{-1} are extremely low, whereas they are growing up again in the q range beyond 90 nm^{-1}. This effect shows clearly the importance of measurements covering an extended q range.

Atomic Distribution Functions

From the structure factors the reduced atomic distribution functions $G(r)$ were evaluated by Fourier transformation.

$$G(r) = 4\pi r[\varrho(r) - \varrho_0] = \frac{2}{\pi}\int_0^{q_m} q[S(q) - 1]\sin(qr)\,dq\,, \qquad (6)$$

where $\varrho(r)$ is the atomic distribution function giving the atomic number density at the distance r from a reference atom at $r = 0$. ϱ_0 is the mean atomic number density, and q_m is the maximum q value of the respective diffraction experiment.

The results are given in Fig. 2, and the atomic distances and coordination numbers extracted from the $G(r)$ functions are listed in Table 1. The curves e and f exhibit more detailed structure than reported up to now in literature for amorphous T–M alloys. The first maximum splits up into two subpeaks, whereas there exist four contributions to the second maximum. Therefore we introduce the following nomenclature: $r_{ij}^{n,m}$ means an atomic distance between a j-type and an i-type atom displayed as m-th subpeak (or shoulder) of the n-th maximum in $G(r)$.

The reduced atomic distribution function $G(r)$ can be represented by the three partial reduced atomic distribution functions

$$G_{ij}(r) = 4\pi r[(1/c_j)\varrho_{ij}(r) - \varrho_0]\,.$$

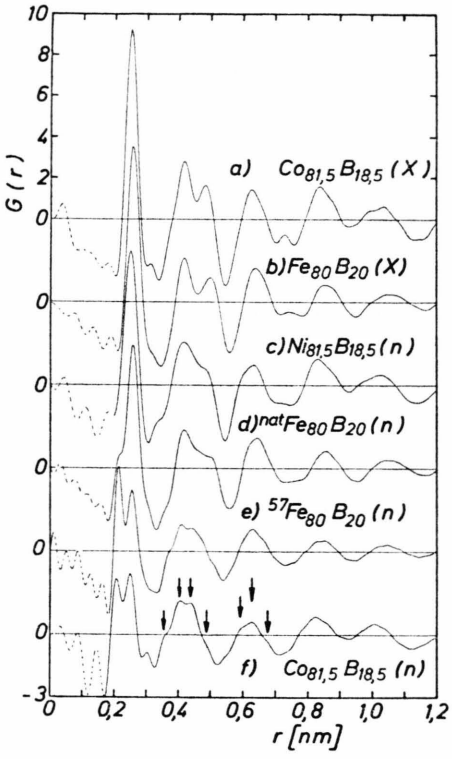

Fig. 2. Reduced atomic distribution functions $G(r)$ of amorphous transition metal-boron alloys. (X) and (n) denote X-ray and neutron scattering, respectively.

ϱ_{ij} means the number of j-atoms per unit volume at the distance r from an i-atom.

$$G(r) = \frac{c_T^2 f_T^2}{\langle f\rangle^2} G_{TT}(r) + \frac{c_B^2 f_B^2}{\langle f\rangle^2} G_{BB}(r) + \frac{2 c_T c_B f_T f_B}{\langle f\rangle^2} G_{BT}(r) = w_{TT} G_{TT}(r) + w_{BB} G_{BB}(r) + 2 w_{BT} G_{BT}(r)\,. \qquad (7)$$

The corresponding weighting factors w_{ij} in (7) are listed in Table 3. It can be clearly seen that with the different specimens investigated in the present work a range could be covered where these weighting factors show a considerable variation. This is very advantageous for the discussion of the $G(r)$ curves:

In the case of the X-ray curves a and b of Fig. 2 the influence of the boron-boron correlation can be neglected, and the contribution of the boron-metal correlation plays a minor role. Therefore these

Table 3. Weighting factors of the partial reduced atomic distribution functions in Equation (7).

Sample	Radiation	w_{TT}	w_{BB}	$2w_{BT}$
$Co_{81.5}B_{18.5}$	X-ray	0.92	0.001	0.08
$Fe_{80}B_{20}$	X-ray	0.91	0.001	0.08
$Ni_{81.5}B_{18.5}$	neutron	0.78	0.013	0.20
$^{nat}Fe_{80}B_{20}$	neutron	0.74	0.018	0.24
$^{57}Fe_{80}B_{20}$	neutron	0.54	0.07	0.38
$Co_{81.5}B_{18.5}$	neutron	0.45	0.11	0.44

curves mainly represent the metal-metal correlation, and the peaks are attributed to distances between T-atoms (see Table 1). The position of the peak $r_{TT}^{I,2}$ is very close to the Goldschmidt diameter of the respective metal atom (0.25 nm for Co, 0.254 nm for Fe [14]). The first peak is followed by a small hump ($Co_{81.5}B_{18.5}$) or a shoulder ($Fe_{80}B_{20}$), respectively, at $r = 0.31-0.32$ nm, which in the case of $Fe_{80}B_{20}$ has also been reported in [11]. The second maximum shows a pronounced splitting up into two subpeaks. It should be noted that the relative distance between the two subpeaks is greater within $Fe_{80}B_{20}$ than within $Co_{81.5}B_{18.5}$, reflecting again the structural differences which have been observed already with the structure factors. The splitting up of the second maximum for $Fe_{80}B_{20}$ as shown in Fig. 2 is much more pronounced than that reported in [9]. The small intermediate peak between the IIIrd and the IVth maximum (0.73 nm for $Co_{81.5}B_{18.5}$, 0.74 nm for $Fe_{80}B_{20}$) occurs also in Refs. [10, 11] but not in [9].

In the case of the neutron curves c and d, where the scattering factor of the metal is still greater than that of boron, the weighting factor of the B–B correlation is still rather small (Table 3) but the contribution of the boron-metal correlation is now considerable in comparison with the T–T correlation. This contribution shows up in Fig. 2 as broadening at the left hand side of the first peak of $Ni_{81.5}B_{18.5}$ and as a shoulder on the first peak of $Fe_{80}B_{20}$ caused by the smaller first neighbour distance between B- and T-atoms.

Also at the second maximum the influence of the B–T-correlation is observable. The valley between the two T–T subpeaks of the X-ray curves $r_{TT}^{II,2}$ and $r_{TT}^{II,4}$, whose heights have become lower, is now filled up by a B–T atomic distance at $r_{BT}^{II,3}$. With the $Fe_{80}B_{20}$ curve this behaviour is clearer displayed than with the $Ni_{81.5}B_{18.5}$ curve because of the higher r-space resolution due to the more extended q range measurement. The third maximum in c and d shows an asymmetry at its left hand side reflecting a not resolved multiple peak structure. The intermediate peak between the IIIrd and the IVth maximum is still present, but not as distinct as in the X-ray curves.

In the case of the neutron curves e and f, where the scattering factors of the metal atoms are smaller than that of the metalloid atoms, the B–T correlation appears with a weighting factor comparable to the weighting factor of the T–T correlation, and the B–B correlation in these cases shows a weighting factor which amounts up to 10% of

$$(w_{TT} + w_{BB} + 2w_{BT}).$$

The different nearest neighbour distances within T–T pairs, $r_{TT}^{I,2}$, and B–T pairs, $r_{BT}^{I,1}$, are clearly resolved in the first maximum. Concerning the $G(r)$ curve of $Co_{81.5}B_{18.5}$ we wish to make the following remark: The comparison with the $Fe_{80}B_{20}$ curve e leads us to the conclusion that the splitted maximum has a physical meaning, whereas the oscillations below $r = 0.2$ nm are ripples produced by an uncertainty in the evaluation of the measured data with $Co_{81.5}B_{18.5}$.

The atomic diameter of the boron atoms was estimated from the $G(r)$ curves with the equation

$$d_B = 2r_{BT}^{I,1} - r_{TT}^{I,2}, \tag{8}$$

yielding 0.171 nm ($Fe_{80}B_{20}$) and 0.164 nm ($Co_{81.5}B_{18.5}$).

These values are close to the tetrahedral covalent diameter of Boron (0.176 nm) [15].

The second maximum exhibits a very detailed structure with four subpeaks (indicated by arrows in Fig. 2f) the first of them occuring as a shoulder, the second and third as separated peaks and the fourth again as a shoulder. The positions of the peaks displayed as a shoulder were estimated and also listed in Table 1.

In the region of the first shoulder the height of the $G(r)$ curve is clearly enhanced in comparison to curves c and d. From the weighting factors in Table 3 it cannot be decided whether this shoulder is caused by the G_{BT} contribution or by the G_{BB} contribution or by both. Thus in order to gain some information on the boron-boron correlation we must go back to

the structure factors of $^{57}Fe_{80}B_{20}$ and $Co_{81.5}B_{18.5}$ (Figure 1). The additional peak at $q^P = 21.5$ to 21.6 nm^{-1} must be caused by the boron-boron correlation because it is visible only in the curves e and *f*, where the scattering factor of boron is larger than that of the metal. If one assumes that this correlation is a B–B distance separated by T metal atoms without any further correlation between the B atoms at higher distances one can approximate the corresponding scattering contribution by

$$I_{BB}(q) \sim \sin(qr_{BB})/qr_{BB}\,, \tag{9}$$

where the peak at q^P reflects the first maximum of this function at $q^P r_{BB} \sim 7.73$. From this follows the boron-boron distance $r_{BB} = 0.36$ nm. This value is within the range where the shoulder at $r^{II,1}$ on the left hand side of the second main maximum in the $G(r)$ curves e and f in Fig. 2 occurs. But it should be noted that calculations of the partial distribution functions performed at present [16] show that also the G_{BT} correlation has a significant contribution within this r range.

The positions of the peaks at $r_{TT}^{II,2}$ and $r_{TT}^{II,4}$ agree with the positions of the corresponding ones for the X-ray curves a and b, however their heights are lower.

The contribution of the partial $G_{BT}(r)$ function to the total $G(r)$ at $r_{BT}^{II,3}$, which could already be observed at the curves c and d in Fig. 2, is now clearly displayed as a distinct peak in the curves e and f between $r_{TT}^{II,2}$ and $r_{TT}^{II,4}$ in accordance with the increased weighting factor w_{BT}. The asymmetry at the left hand side of the IIIrd maximum mentioned above for the curves c and d exhibits as a shoulder $r^{III,1}$ in the curves e and f, and an additional shoulder $r^{III,3}$ occurs at the right hand side of the maximum (see arrows in Figure 2).

In the following section the evaluation of coordination numbers will be described, which are given in Table 1. N_m^I denotes a measured area under the first peak of the radial distribution function RDF(r)

$$N_m^I = \int \mathrm{RDF}(r)\,\mathrm{d}r = \int 4\pi r^2 \varrho(r)\,\mathrm{d}r \tag{10}$$

taken from minimum to minimum.

Excluding B–B nearest neighbours, $\varrho(r)$ can be written for the r range of the first maximum:

$$\varrho^I(r) = \frac{w_{TT}}{c_T}\varrho_{TT}(r) + 2\frac{w_{BT}}{c_T}\varrho_{BT}(r)\,, \tag{11}$$

and in terms of coordination numbers

$$N_m^I = \frac{w_{TT}}{c_T} z_{TT}^I + 2\frac{w_{BT}}{c_T} z_{BT}^I\,, \tag{12}$$

where z_{ij}^I is the number of j-type atoms sourrounding an i-type atom within the first coordination shell. In the case of the neutron curves e and f, the coordination numbers z_{TT} and z_{BT} can be estimated from the areas $N_m^{I,1}$ and $N_m^{I,2}$ of the two subpeaks. If one assumes as an approximation that $\varrho_{TT}(r)$ is negligibly small in the region of the B–T subpeak and that $\varrho_{BT}(r)$ is small in the region of the T–T subpeak, (12) can be splitted up:

$$N_m^{I,1} = 2\frac{w_{BT}}{c_T} z_{BT}^I\,, \tag{13a}$$

$$N_m^{I,2} = \frac{w_{TT}}{c_T} z_{TT}^I\,. \tag{13b}$$

The partial coordination numbers z_{TT}, z_{BT}, and $z_{TB} = z_{BT} c_B/c_T$ were derived from the measured peak areas and listed in Table 1. There occurs a difference between the values for $Co_{81.5}B_{18.5}$ and those for $Fe_{80}B_{20}$, which is a further indication on a different structural behaviour of these two substances:

As a cross check with the partial coordination numbers, the first peak areas N_c^I were calculated with (12) for the X-ray curves of $Co_{81.5}B_{18.5}$ and $Fe_{80}B_{20}$ and also for the neutron curve of $^{nat}Fe_{80}B_{20}$ (see Table 1). It can be seen that the agreement between the calculated N_c^I and the measured N_m^I is better than one atom in all cases.

Acknowledgements

Thanks are due to the Kernforschungszentrum Karlsruhe for the allocation of beam time at the research reactor FR2, and to the Institute Laue-Langevin for the allocation of beam time at the high flux research reactor. This work was partly supported by the Deutsche Forschungsgemeinschaft, Bad Godesberg, and the Verein Deutscher Giessereifachleute, Düsseldorf.

[1] H. F. Bühner and S. Steeb, Z. Metallkde. **62**, 27 (1971).
[2] R. Hezel and S. Steeb, Phys. Kond. Materie **14**, 314 (1972).
[3] J. Krogh Moe, Acta Cryst. **9**, 951 (1956).
[4] H. H. Paalmann and C. J. Pings, J. Appl. Phys. **33**, 2635 (1962).
[5] G. E. Bacon, Neutron Diffraction, 3rd ed., at the Clarendon Press, Oxford 1975.

[6] According to measurements with sputtered films. A. Brunsch, IBM Deutschland GmbH, private communication.
[7] V. F. Sears, Adv. Phys. **24**, 1 (1975).
[8] J. Blétry and J. F. Sadoc, J. Phys. F: Metal Phys. **5**, L 110 (1975).
[9] Y. Waseda and H. S. Chen, Phys. Stat. Sol. (a) **49**, 387 (1978).
[10] K. Suzuki, F. Itoh, M. Misawa, M. Matsuura, and T. Fukunaga, Suppl. Sci. Rep. RITU, **A 28**, 12 (1980).
[11] W. A. Rathbun and C. N. J. Wagner, M. S. Thesis, UCLA (1978).
[12] N. Cowlam, M. Sakata, and H. A. Davies, J. Phys. F.: Metal Phys. **9**, L 203 (1979).
[13] G. S. Cargill III, Solid State Phys. **30**, 227 (1975).
[14] W. Hume Rothery and G. V. Raynor, The Structure of Metals and Alloys, 3rd ed., London, Inst. Metals, 1954.
[15] L. Pauling, The Nature of the Chemical Bond, 3rd ed., Cornell Univ. press, Ithaca, New York 1960, p. 246.
[16] E. Nold et al, to be published.